

# Green Synthesis of Bovine Serum Albumin Conjugated Silver Nanoparticles at Different Temperatures and Evaluation of Their Antioxidant Activity

MAHESWARI BEHERA\*, SIBA SOREN<sup>1</sup>, NIHAR RANJAN SINGH, B. S. SIPRA, GANGADHAR SETHI<sup>2</sup>, SMRUTI MAHANANDIA<sup>3</sup>, BISWAJITA PRADHAN<sup>4</sup> AND MADHABI MADHUSMITA BHANJADEO

Department of Botany, Ravenshaw University, Cuttack 753003, <sup>1</sup>Department of Chemistry, Government Women's College, Baripada 757001, <sup>2</sup>Department of Botany, Shailabala Women's Autonomous College, Cuttack 753001, <sup>3</sup>College of Basic Science and Humanities, Orissa University of Agriculture and Technology (OUAT), Bhubaneswar 751003, <sup>4</sup>School of Biological Sciences, Asian Institute of Public Health (AIPH) University, Bhubaneswar, Odisha 752101, India

## Behera *et al.*: Green Synthesized Bovine Serum Albumin-Silver Nanoparticles as an Antioxidant Molecule

Over the past few years, nanotechnology has become an incredibly captivating field of research in science and technology. Due to their superior optical, chemical, photo-electrochemical, and electronic properties over their bulk counterparts, nanomaterials are being used as the cornerstones of nanoscience. The use of different nanostructured materials has revolutionized technology in the field of biology, industry, and medicine. Many bio-molecules like proteins, nucleic acids, and lipids coalesce with nanoparticles in biological systems with minimal toxicity. In this context, circulating protein molecules like albumin can be used as a scaffold for generating an array of nanoparticles for biomedical purposes such as delivery agents for therapeutic use. Albumin protein found in human blood has no immunogenicity as an endogenous protein and ensures its biocompatibility for albumin-based nanoparticles. In the present study, the interaction between silver nanoparticles synthesized from *Ocimum sanctum* leaves and bovine serum albumin protein is carried out under differential temperatures to evaluate the physicochemical characterization of this formed complex. For this purpose, silver nanoparticles are prepared by the bioreduction method and allowed to interact with the native bovine serum albumin. Different *in vitro* antioxidant assays of the synthesized nanocomposites were also carried out. Hence, exploring the effects of interaction between green synthesized nanoparticles and bovine serum albumin can be useful for designing nanomaterials for nanoscale drug delivery applications in biological systems.

**Key words:** Silver nanoparticles, bovine serum albumin, nanoparticles-protein interaction, antioxidant activity

Nanoparticles and nanomaterials have emerged as dominant technological implementations in the human health sector for different therapeutic as well as diagnostic applications<sup>[1]</sup>. Due to their encouraging physical and chemical characteristics, as well as their ability to be compatible with living organisms, they have been widely investigated as nanoprobe for identifying diseases, nanocarriers for delivering drugs in a controlled and targeted manner, devices for loading drugs on a nanoscale, and vehicles for transferring specific genes or messenger Ribonucleic Acid (mRNA) molecules<sup>[2]</sup>. Out of different groups of nanomaterials predominantly Silver Nanoparticles (SNPs) have gained more attention for their biocompatibility and versatility and are exploited for

a wide group of biological applications<sup>[3]</sup>. In the past decade, there was an exponential surge in the green synthesis of silver and other metal nanoparticles because of their sustainability and economic potential. Specifically, plants as a whole, plant-based materials, and plant extracts have been in greater use for the green synthesis of SNPs over other biological means<sup>[4]</sup>. This trend was possibly due to two principal factors that provide an advantage over

This is an open access article distributed under the terms of the Creative Commons Attribution-NonCommercial-ShareAlike 3.0 License, which allows others to remix, tweak, and build upon the work non-commercially, as long as the author is credited and the new creations are licensed under the identical terms

Accepted 21 October 2024

Revised 25 April 2024

Received 18 March 2023

Indian J Pharm Sci 2024;86(5):1690-1701

\*Address for correspondence

E-mail: beheramaheswari97@gmail.com

other means for the synthesis of SNPs. The first one is the precision and maintaining the specific order in the shapes and sizes offered by plant metabolites<sup>[5]</sup>. The second factor is the enhanced rate of reaction after seeding as compared to other organism-based synthesis. The role of reducing equivalent secondary metabolites present in plants plays a vital role in both the controllability of shapes while maintaining the inter-atomic distances as well as the rapid rate of reaction of synthesis. However, the interaction of SNPs with various bio-molecules has come into view as the essential cue for biomedical applications<sup>[6]</sup>. Biomolecules like proteins, nucleic acids, antibodies, and lipoprotein conjugates are reported as candidates for probing against the detection of disease, and delivery of targeted drugs or genes<sup>[7]</sup>. Along with these biomolecule-associated nanoparticles are investigated for novel therapeutic approaches like photodynamic therapy and photothermal therapy<sup>[8]</sup>. Out of diverse biomolecules plasma proteins like serum albumin are considered crucial molecules for applications like nano-medicines and controlled drug loading and delivery. When introduced into the bloodstream the nanoparticles rapidly start interacting with the plasma proteins like serum albumin forming a definite structure called the protein corona. The qualitative and quantitative properties of the corona are determined by the physicochemical features of both nanoparticles and serum albumin<sup>[9]</sup>. For nanoparticles to be used as therapeutic agents *in vitro* or *in vivo* settings, a thorough understanding of their interaction mechanism is imperative<sup>[10]</sup>. In the recent past, studies on thermodynamic parameters of Human Serum Albumin (HSA) and SNP interaction revealed possible acting forces and the order of HSA binding to SNP<sup>[11]</sup>. Temperature plays a vital role in stabilizing as well as adding convolution to the albumin structure when interacting with SNPs.

In addition, free radicals have a significant function in biological systems. They participate in essential cellular processes such as cell respiration, but they also contribute to the aging process and the development of various diseases<sup>[12,13]</sup>. Free radicals are molecules that lack stability due to their unpaired electrons, making them highly reactive and capable of causing damage to the biomolecules within our bodies<sup>[14-16]</sup>. In organisms that require oxygen, free radicals are generated through regular metabolic activities<sup>[17]</sup>. Mitochondria are the key culprits of oxidative damage as they can release free radicals like superoxide from the electron transport

chain<sup>[18,19]</sup>. To avoid harm caused by free radicals within cells, an internal antioxidant system has been established. This mechanism utilizes proteins to transform free electrons into a stable, non-reactive state. Antioxidants manage oxidative reactions by obstructing, slowing down, or impeding the oxidation of biomolecules<sup>[20]</sup>. Certain components of critical antioxidant enzymes provide a safeguard and preservation for proteins<sup>[21,22]</sup>. Non-enzymatic antioxidants can also neutralize radicals<sup>[23,24]</sup>. Recent reports suggest that artificial antioxidants, including Butylated Hydroxytoluene (BHT) and Butylated Hydroxyanisole (BHA), may pose risks to human health<sup>[25-27]</sup>. Consequently, the quest for natural compounds with antioxidative capabilities that are both efficient and safe has intensified in recent times<sup>[28-37]</sup>. Additionally, nanomaterials have emerged as a crucial factor in human well-being and healthcare due to their significant advantages in biomedical applications<sup>[38-42]</sup>. Furthermore, some nanomaterials have demonstrated a potent antioxidant capacity, which presents an intriguing possibility for creating novel therapies with more focused and improved effects. For instance, gold, silver (Ag), and selenium nanoparticles have been found to effectively reduce oxidative stress by functioning as efficient scavengers of redox-active radicals<sup>[43-46]</sup>.

*Ocimum sanctum* (*O. sanctum*) L., commonly known as holy basil or tulsi is native to the Indian subcontinent. It has been a well-known medicinal plant since time immemorial, in addition to its enormous religious sanctity.

Hence, in this work, SNPs were synthesized using *O. sanctum* leaf extract using a green synthesis approach. The synthesized SNPs interacted with native Bovine Serum Albumin (BSA) and different physicochemical characteristics were evaluated under different temperatures. Furthermore, the *in vitro* antioxidant activities of the nano-composites were also investigated.

## MATERIALS AND METHODS

### Chemicals and plant materials:

Silver nitrate (AgNO<sub>3</sub>), tris base, glycerol, and brilliant blue were obtained from HiMedia Laboratories Pvt. Ltd., Mumbai. Potassium hydroxide (KOH), acetone, acrylamide, N'N'-bis-methylene-acrylamide, bromophenol blue, Trichloroacetic Acid (TCA), BHT, ascorbic acid, and Hydrogen peroxide (H<sub>2</sub>O<sub>2</sub>) were procured from Sisco Research Laboratories Pvt., Ltd.

(SRL), Maharashtra; BSA from Central Drug House (CDH), New Delhi; Potassium bromide (KBr), Safety Data Sheets (SDS) from Merck, Mumbai; Ammonium persulfate (APS) and Tetramethylethylenediamine (TEMED) from Bio-Rad Laboratories. The leaves of holy basil (*O. sanctum* L.) were collected from the garden of the Department of Botany, Ravenshaw University.

#### Preparation of plant extract:

20 g of fresh leaves from *O. sanctum* were collected and washed thoroughly with distilled water before extraction. Leaves were finely cut into small pieces and 100 ml of distilled water was added followed by boiling at 60° for 1 h. The mixture was then cooled and filtered with Whatman paper No. 1 and stored at 4° for further analysis<sup>[47]</sup>.

#### Preparation of BSA solution:

The stock solutions of BSA (10 mg/ml) were prepared in double distilled water. From stock solution, the working solution of BSA (1 mg/ml) was used in all the experiments<sup>[47]</sup>.

#### Synthesis of SNPs from plant leaf extract:

200 µl of aqueous *Ocimum* leaf extract on which 1 mM of 50 µl of AgNO<sub>3</sub> solution was added. The final volume was made up to 10 ml by adding double distilled water. 0.01 M KOH solution was added to make the mixture slightly alkaline. The mixture was stirred at 150 revolutions per minute (rpm) on a magnetic stirrer over a hot plate at 30°, 40°, 60°, 80°, and 100°. A change in the color of the reaction mixture within 5 to 30 min was observed<sup>[48]</sup>. This reaction mixture was either incubated with BSA solution or stored at 4° for further use.

#### Incubation of SNPs in BSA solution:

The SNPs thus formed from *Ocimum* leaf extract using the bioreduction method were incubated with the working BSA (1 mg/ml) solution<sup>[49]</sup>. This mixture of solutions containing SNPs and BSA was stored at 4° before physicochemical characterization studies.

#### Characterization:

Different analytical characterization like Ultraviolet (UV)-visible spectral analysis, fluorescence spectral analysis, Scanning Electron Microscopy (SEM), Fourier Transform Infrared (FTIR), and Sodium Dodecyl Sulfate Polyacrylamide Gel Electrophoresis (SDS-PAGE) analysis of synthesized SNPs and SNP-BSA

complex was done to evaluate the physicochemical properties<sup>[47-49]</sup>.

#### Antioxidant assay:

**1,1-Diphenyl-2-Picrylhydrazyl (DPPH) radical scavenging assay:** The DPPH scavenging potential of the SNPs, BSA, and BSA conjugated SNP was determined using the method of Mensor *et al.*<sup>[50]</sup>. Ascorbic acid was a positive control. 1 ml of DPPH solution was added with 800 µl of tris-Hydrochloride (tris-HCl) buffer (pH 7.4) in a test tube and then 200 µl of testing sample solution was added and mixed quickly followed by incubating it at room temperature for 30 min. The absorbance of the solution at 517 nm was recorded. A mixed solution with 1200 µl of ethanol and 800 µl of tris HCl buffer (pH 7.4) was used as the blank while ascorbic acid acted as the positive control. The inhibition ratio (%) was obtained from the following equation.

$$\text{Inhibition ratio (\%)} = (A_1 - A_2) \times 100 / A_1$$

Where, A<sub>1</sub> is the absorbance of the blank and A<sub>2</sub> is the absorbance of the testing sample solution.

#### 2,2'-Azino-Bis(3-Ethylbenzothiazoline-6-Sulfonic acid) (ABTS) assay:

To conduct the ABTS assay, we used the protocol established by Re *et al.*<sup>[51]</sup>. BHT was used as a positive control. Briefly, an initial reaction volume of 2.7 ml was prepared by adding 0.3 ml of testing samples in 10 % Dimethyl Sulfoxide (DMSO) to the diluted ABTS. The control sample contained 0.30 ml of 10 % DMSO and 2.70 ml of ABTS. The absorbance at 734 nm was measured after the sample was incubated for 60 min at room temperature and in the dark. BHT was used as the positive control. To determine the percentage of inhibition, the following equation was used.

$$\text{Percent of inhibition} = ((\text{Optical Density (OD) (control)} - \text{OD (sample)}) / \text{OD (control)}) \times 100$$

#### Superoxide radical scavenging activity:

The superoxide radical scavenging activity was determined by Patel *et al.*<sup>[52]</sup>. The use of ascorbic acid served as a positive control. Briefly, the 3 ml reaction mixture consists of 0.01 M phosphate buffer (pH 7.8), 0.5 mM Ethylenediaminetetraacetic acid (EDTA), Nitroblue Tetrazolium (NBT) (0.75 mM), 20 µg riboflavin, and varying concentration of testing samples for 6 min. As a control, methanol was employed.

### H<sub>2</sub>O<sub>2</sub> scavenging activity:

Ruch *et al.*<sup>[53]</sup> suggested a method for H<sub>2</sub>O<sub>2</sub> scavenging. Blanks included phosphate buffer and H<sub>2</sub>O<sub>2</sub>. The positive control was ascorbic acid. Briefly, 1 ml of various testing samples was mixed with 40 mM H<sub>2</sub>O<sub>2</sub> and 2.4 ml 1 M phosphate buffer (pH 7.4). After 10 min of incubation, the absorbance was measured at 230 nm. Blanks included phosphate buffer and H<sub>2</sub>O<sub>2</sub>. The positive control was ascorbic acid.

### Hydroxyl (-OH) radical scavenging activity:

The -OH radical scavenging capacity was measured using the modified method as described previously de Avellar *et al.*<sup>[54]</sup>. Ascorbic acid was used as a positive control (1 mg/ml). Briefly, the reaction mixture contained deoxyribose (2.8 mM), Potassium dihydrogen phosphate (KH<sub>2</sub>PO<sub>4</sub>)-Sodium hydroxide (NaOH) buffer, pH 7.4 (0.05 M), Ferric chloride (FeCl<sub>3</sub>) (0.1 mM), EDTA (0.1 mM), H<sub>2</sub>O<sub>2</sub> (1 mM) and different concentrations of the testing samples in a final volume of 2 ml. The mixture was incubated at 37° for 30 min followed by the addition of 2 ml of TCA (2.8 % w/v) and thiobarbituric acid. Thereafter it was kept for 30 min in a boiling water bath and cooled. The absorbance was recorded at 532 nm in a UV-visible spectrophotometer.

## RESULTS AND DISCUSSION

The formation of SNPs from *O. sanctum* leaf extract was primarily observed from the color change of the solution. The color change in the reaction mixture indicates the formation of SNPs that were generated by the reduction of AgNO<sub>3</sub>. The activation of surface plasmon vibrations gives SNPs their distinctive golden yellow color as shown in fig. 1 at 40° to 100° temperature range. This change in the color of the reaction mixture indicates that the silver ions in the reaction medium have been transformed into elemental silver with a nanometric size. To achieve such conversions, reducing entities in the reaction media is always required. The biomolecules found in *O. sanctum* leaf extract operate as a reducing agent in this case. The same color change pattern was also reported by researchers<sup>[47,55]</sup>. However, we observed that there was no significant color change in the mixture at temperatures 4° and 30°. From this, it is concluded that the SNPs might not be synthesized in this temperature range using *O. sanctum* leaf extract.

From fig. 2, it was observed that the pH value of both the reaction mixtures containing the SNPs and SNP-BSA complexes gradually decreases as the temperature rises from 40° to 100°. It may be due to the release of more H<sup>+</sup> ions into the solution with an increase in temperature.

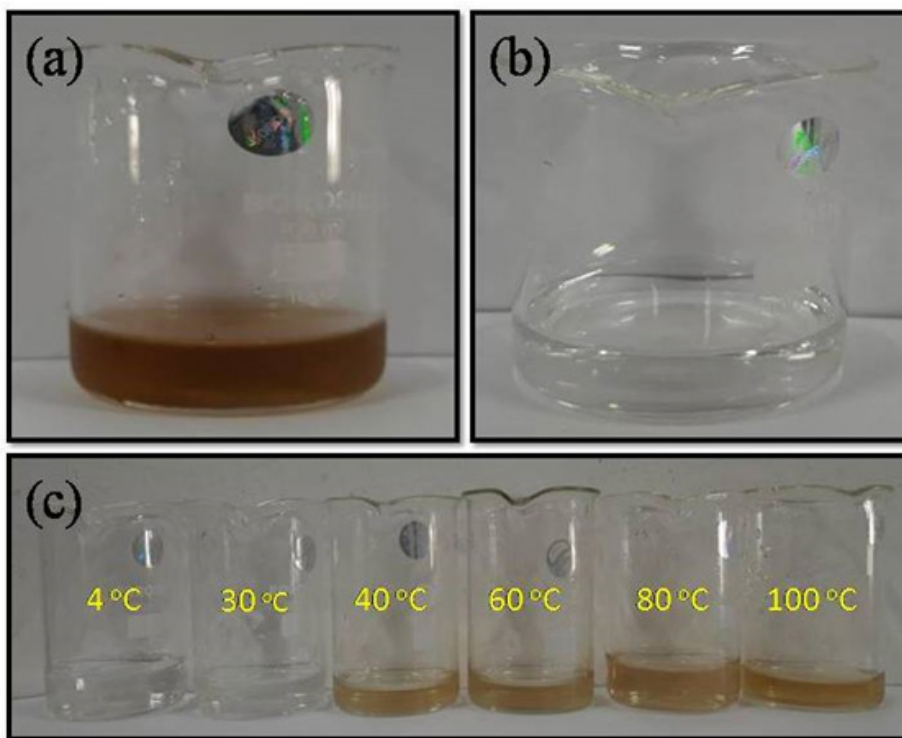
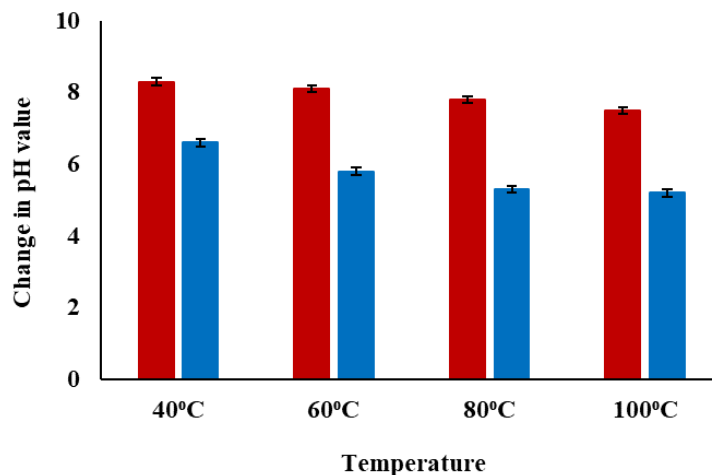


Fig. 1: Leaf extract of (a): *O. sanctum* L.; (b): 1 mM AgNO<sub>3</sub> solution and (c): Synthesis of SNPs at different temperatures



**Fig. 2: Graph showing the change in pH value**

Note: (■): Observed pH value of SNP solutions and (■): Observed pH value of SNP+BSA solutions

From the UV-visible spectral analysis in fig. 3, it is observed that BSA shows a maximum absorbance peak at 280 nm. According to previous studies<sup>[47,55]</sup>, an absorption peak between 400-420 nm indicates the formation of SNPs. No spectral peaks were observed in the solution containing SNPs synthesized at 4° and 30° indicating the possibility of the non-existence of SNPs at these temperatures. It has been observed that there is an increase in the absorbance value of SNPs with an increase in temperature. It might be due to an increase in the concentration of SNPs in the reaction mixture. The possible explanation may be that an increase in temperature provides a favorable condition for the formation of a greater number of SNPs. When BSA was incubated with SNP in an equal ratio, an absorption peak was detected between 310 nm and 320 nm, and no separate absorption peaks for BSA and SNP were observed. It occurred due to the possible interaction that happened between the BSA and SNPs leading to the formation of a nanocomposite consisting of both BSA and SNP.

As depicted in fig. 4, the fluorescence emission intensity of native BSA was found to be maximum at 320-360 nm. With increasing temperature, the fluorescence emission intensity of the BSA-SNP complex steadily decreased up to four times as seen in between native BSA and BSA-SNP complex synthesized at 100°. As a result, the SNP in the SNP-BSA complex may be considered a quencher molecule that causes a drop in the fluorescence emission intensity. In a similar experiment, Mariam *et al.*<sup>[49]</sup> reported a decrease in fluorescence emission intensity for BSA incubated with chemically synthesized SNPs indicating a considerable quenching affinity of SNP towards BSA's intrinsic fluorescence.

From the SEM images of fig. 5, spherical SNPs were observed in a reaction mixture containing SNPs and SNP-BSA complex at different temperatures. With the increase in the temperature, the size of the SNPs was found to be increased whereas there is a visible rise in the aggregation of SNPs over the structure of the BSA protein in the SNP-BSA reaction mixture. It is to be noted that at such high temperatures, the proteins like BSA may undergo denaturation and the association of SNPs over the protein surface may play a crucial role in our understanding of protein-SNP dynamics.

In fig. 6, the FTIR spectrum observed in SNPs and native BSA was found to be distinct whereas the spectral pattern in the SNP-BSA complex at different temperatures was found to be varied when compared to the SNP and native BSA. Particularly, in the range of the wavenumber from 2000 to 500, a clear peak was observed for SNP-BSA at 40° whereas no such peaks were seen in the SNP-BSA reaction mixture at 60°, 80° and 100°. This might be due to the effect of high temperature on the three-dimensional conformation of the protein structure.

In the SDS-PAGE analysis in fig. 7, no bands were seen for SNPs. On the other hand, the BSA and the SNP-BSA complex at different temperatures show the protein bands around the molecular weight of BSA. The order of migration of the protein band was found to be SNP-BSA complex (100°)>SNP-BSA complex (80°)>SNP-BSA complex (60°)>SNP-BSA complex (40°). It may be concluded that the increase in migration may be due to the accumulation of anionic character (charges) or change in pH or change in the mass or shape of the molecule.

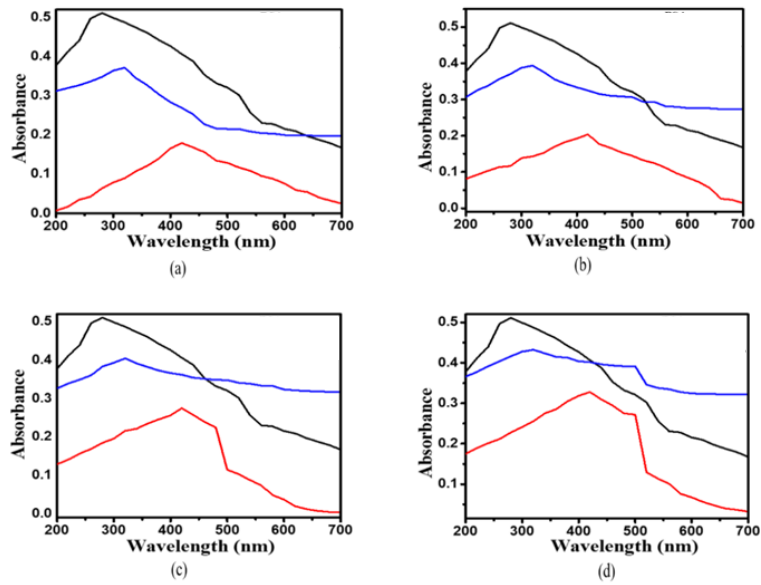


Fig. 3: UV-Vis spectral analysis of BSA; NSP synthesized and its incubation with BSA solution at, (a): 40°; (b): 60°; (c): 80° and (d): 100°  
 Note: (—): BSA; (—): SNP 100° and (—): SNP 100°+BSA

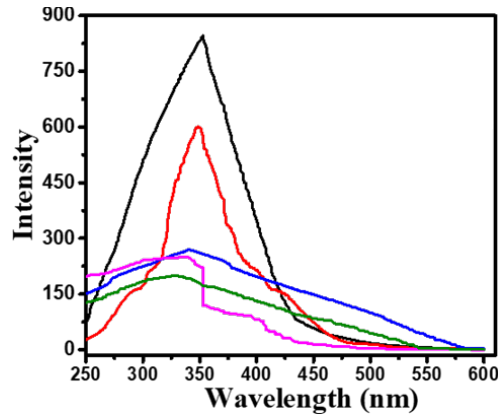


Fig. 4: Fluorescence intensity of BSA and BSA incubated with SNPs synthesized at different temperatures  
 Note: (—): BSA; (—): SNP 40°+BSA; (—): SNP 60°+BSA; (—): SNP 80°+BSA and (—): SNP 100°+BSA

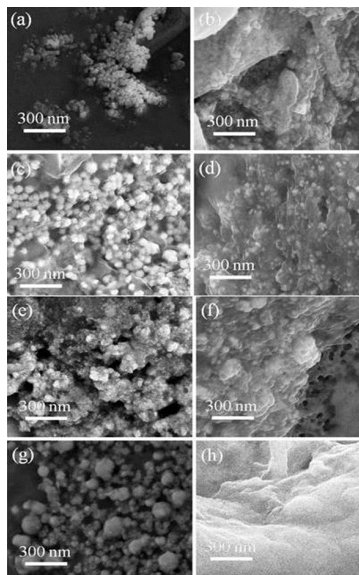
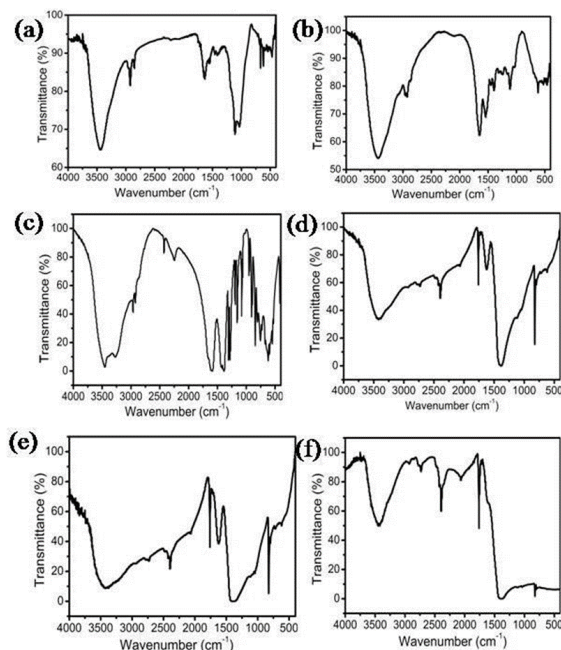
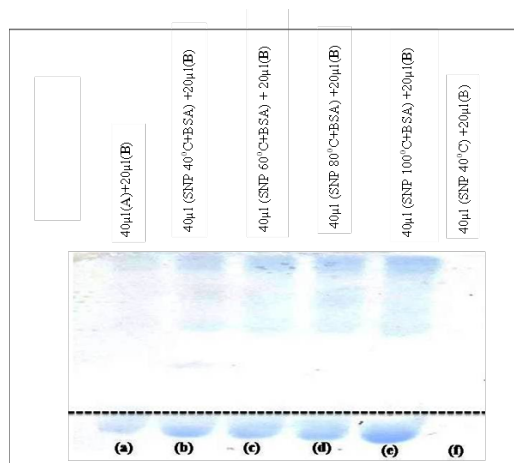


Fig. 5: SEM image, (a): SNP at 40°; (b): SNP-BSA at 40°; (c): SNP at 60°; (d): SNP-BSA at 60°; (e): SNP synthesized at 80°; (f): SNP-BSA at 80°; (g): SNP at 100° and (h): SNP-BSA at 100°



**Fig. 6:** FTIR graph, (a): Synthesized SNP; (b): Native BSA; (c): SNP-BSA at 40°; (d): SNP-BSA at 60°; (e): SNP-BSA at 80° and (f): SNP-BSA at 100°



**Fig. 7:** SDS-PAGE profile of SNP and SNP-BSA synthesized at different temperatures, (a): BSA solution (1 mg/ml); (b): SNP-BSA complex (100°); (c): SNP-BSA complex (80°); (d): SNP-BSA complex (60°); (e): SNP-BSA complex (40°) and (f): Sample buffer

To evaluate the antioxidant potential of the SNP-BSA complex synthesized at different temperatures, various *in vitro* antioxidant assays were performed (fig. 8-fig. 12). In all the assays, a similar pattern of results has been obtained. As previously reported, BSA and all the standard antioxidants used like ascorbic acid and BHT showed free radical scavenging activities<sup>[13,29,56-61]</sup>. Among all the SNPs and SNP-BSA composites synthesized at various temperature conditions, both SNP and SNP-BSA complexes synthesized at 40° showed the highest antioxidant activity in a dose-dependent manner. However, the scavenging activity of both SNPs and SNP-BSA complex is gradually decreasing from 40° to 100°. This might be due to the production of smaller shaped nanoparticles at 40°

which exhibited the free radical scavenging activity effectively. Research has also shown that the high ratio of surface area to volume in nanoparticles is crucial in their ability to counteract free radicals<sup>[62]</sup>.

Owing to the inherent characteristic feature of SNPs, produced using the green synthesis method possesses remarkable applications in multidisciplinary fields like diagnosis, drug delivery, and fabrication of nanobiomaterials. Green synthesis of SNPs using plant materials provides a better alternative when compared to conventional methods. This is not only naturally derived from bio-sources, but also free from hazardous chemicals and sustainable for biological and medical uses. Many attempts were made and evaluated on the

feasibility of synthesis of nano-biomaterials by using biomolecules like proteins and nucleic acids aggregated with nanoparticles that may provide suitable stabilizing, reducing, and capping materials. The optimum temperature for interaction between nanoparticles and biomolecules may play a crucial role in the preparation of sustainable and useful bio nano-materials using a

green synthesis approach. The synthesis of nanoparticles using the extract of tulsi leaves and incubating such synthesized nanoparticles with BSA provides a better platform for large-scale production, easy availability of materials, rapid preparation, and environmentally benign and diverse biomedical applications.

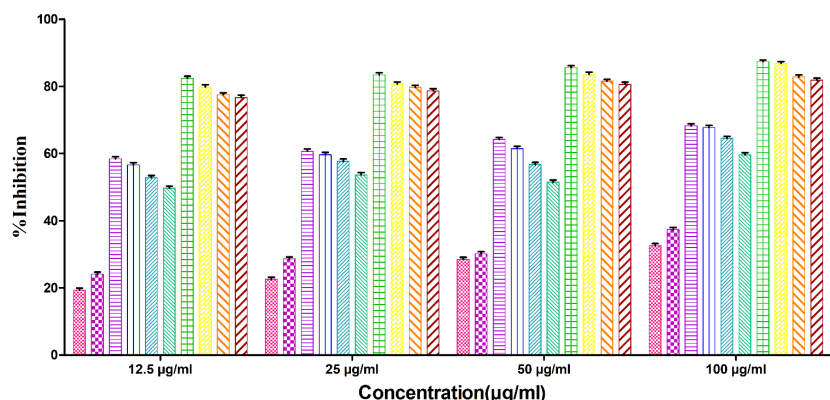


Fig. 8: DPPH assay of ascorbic acid, BSA, SNP, and SNP-BSA complex at different temperatures

Note: (■): Ascorbic acid; (■): BSA; (■): SNP (40°); (■): BSA+SNP (40°); (■): SNP (60°); (■): BSA+SNP (60°); (■): SNP (80°); (■): BSA+SNP (80°); (■): SNP (100°) and (■): BSA+SNP (100°)

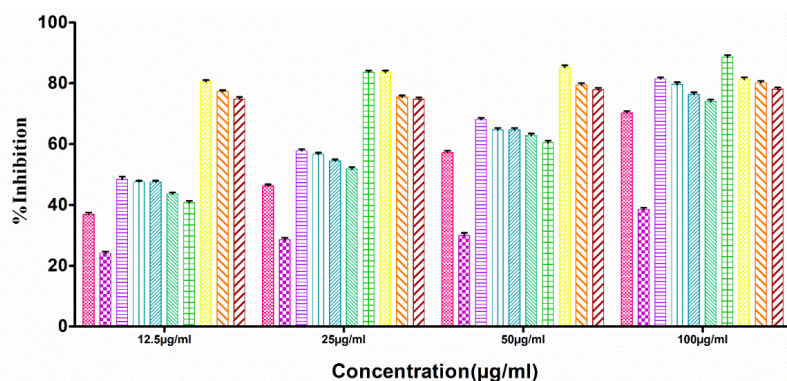


Fig. 9: ABTS assay of ascorbic acid, BSA, SNP, and SNP-BSA complex at different temperatures

Note: (■): BHT; (■): BSA; (■): SNP (40°); (■): BSA+SNP (40°); (■): SNP (60°); (■): BSA+SNP (60°); (■): SNP (80°); (■): BSA+SNP (80°); (■): SNP (100°) and (■): BSA+SNP (100°)

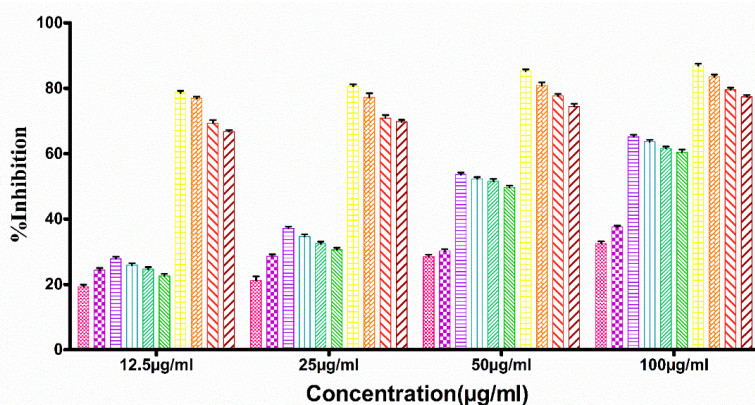


Fig. 10: Superoxide radical scavenging assay of ascorbic acid, BSA, SNP, and SNP-BSA complex at different temperatures

Note: (■): Ascorbic acid; (■): BSA; (■): SNP (40°); (■): BSA+SNP (40°); (■): SNP (60°); (■): BSA+SNP (60°); (■): SNP (80°); (■): BSA+SNP (80°); (■): SNP (100°) and (■): BSA+SNP (100°)



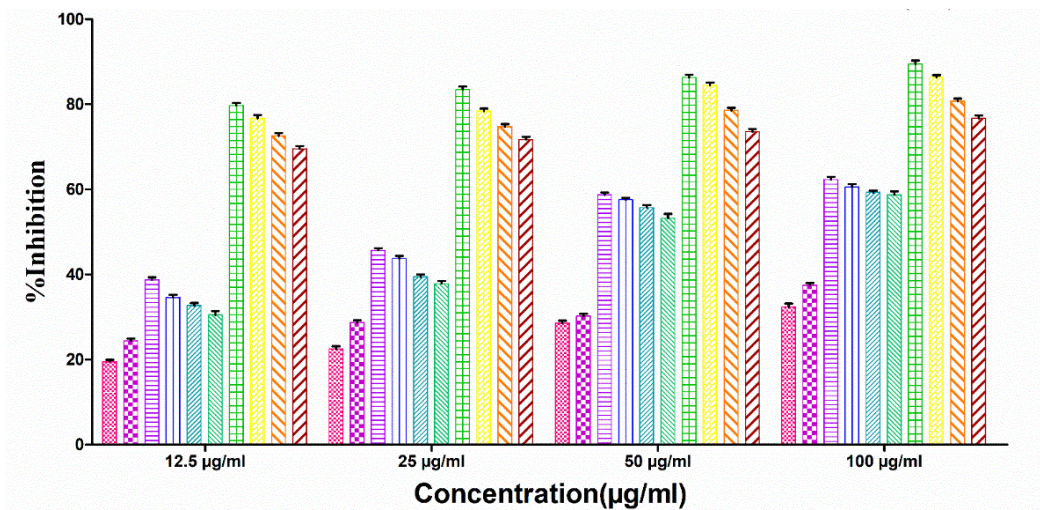


Fig. 11: H<sub>2</sub>O<sub>2</sub> scavenging assay of ascorbic acid, BSA, SNP, and SNP-BSA complex at different temperatures

Note: (■): Ascorbic acid; (■): BSA; (■): SNP (40°); (■): BSA+SNP (40°); (■): SNP (60°); (■): BSA+SNP (60°); (■): SNP (80°); (■): BSA+SNP (80°); (■): SNP (100°) and (■): BSA+SNP (100°)

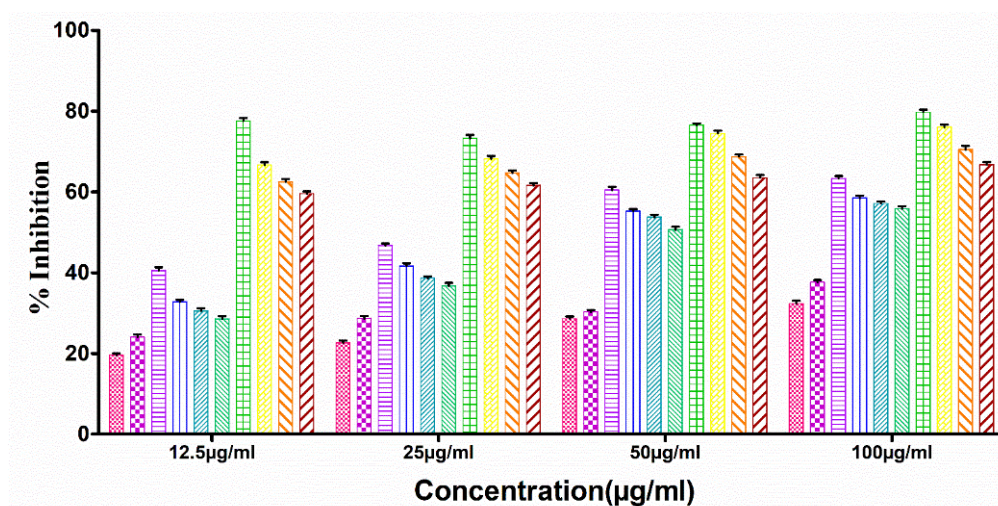


Fig. 12: Hydroxyl radical scavenging assay of ascorbic acid, BSA, SNP, and SNP-BSA complex at different temperatures

Note: (■): Ascorbic acid; (■): BSA; (■): SNP (40°); (■): BSA+SNP (40°); (■): SNP (60°); (■): BSA+SNP (60°); (■): SNP (80°); (■): BSA+SNP (80°); (■): SNP (100°) and (■): BSA+SNP (100°)

Evaluating the optical and physicochemical characterization of green synthesized SNPs, the color change of the reaction mixture conforms to the formation of SNPs. Further, under a UV-visible spectrophotometer, these nanoparticles show an absorption peak at 400-420 nm that authenticates the presence of nanoparticles. When these naturally synthesized SNPs are incubated with BSA, the absorption peak shifts towards a lower wavelength indicating the formation of the nanoparticles-protein complex. Furthermore, the analysis of fluorescence spectrum and intensity analyses show that the SNPs have a considerable ability to quench the intrinsic fluorescence of BSA. From SEM analysis, it was observed that the nanoparticles are roughly spherical and BSA acts as a template for nanoparticles as all

the nanoparticles get bound to the surface of BSA. FTIR result shows that there is a change in the peak which indicates some conformational change in protein structure. Further, the electrophoretic migration result shows the higher migration rate of the SNP-BSA complex formed at 100°, suggesting changes in the protein conformations due to the binding of SNPs.

Both SNPs and SNP-BSA complexes had high antioxidant activity *in vitro*, and their antioxidant capacity increased with the increased concentrations. SNPs and SNP-BSA complex synthesized at 40° showed high antioxidant activity as compared to other temperatures. This may be due to the synthesis of small-sized nanoparticles at 40°.

Hence, this study provides a platform to explore more potential in the green synthesis of protein-nano particles complex and their physicochemical characterization at variable temperatures may be implemented in the field of environmental and health science. Again, the nanoparticle-protein complex synthesized using green methods has the potential to serve as a natural antioxidant source and may hold significant value as a therapeutic agent in the prevention or treatment of diseases related to oxidative stress.

### Acknowledgements:

The authors are thankful to the Department of Botany, Ravenshaw University, Cuttack, Odisha, India; Department of Chemistry, Government Women's College, Baripada, Odisha, India; Shailabala Women's Autonomous College, Cuttack, Odisha, India; College of Basic Science and Humanities, Orissa University of Agriculture and Technology (OUAT), Bhubaneswar, Odisha, India; and Asian Institute of Public Health (AIPH) University, Bhubaneswar, Odisha, India for providing the necessary infrastructure for conducting this research.

### Conflict of interest:

The authors declared no conflict of interests.

### REFERENCES

1. Yuan Y, Zhang F, Wang Y, Li X, Zhao R, Shao D, *et al.* Determination of spectinomycin by SERS based on BSA-protected AgNPs decorated with  $\alpha$ -CD. *Microchem J* 2022;172:106938.
2. Hashemnia S, Zarei H, Mokhtari Z, Mokhtari MH. An investigation of the effect of PVP-coated silver nanoparticles (SNPs) on the interaction between clonazepam and bovine serum albumin based on molecular dynamics simulations and molecular docking. *J Mol Liquids* 2021;323:114915.
3. Khan SA, Shahid S, Lee CS. Green synthesis of gold and silver nanoparticles using leaf extract of *Clerodendrum inerme*; characterization, antimicrobial, and antioxidant activities. *Biomolecules* 2020;10(6):835.
4. Morales-Lozoya V, Espinoza-Gómez H, Flores-López LZ, Sotelo-Barrera EL, Núñez-Rivera A, Cadena-Nava RD, *et al.* Study of the effect of the different parts of *Morinda citrifolia* L.(noni) on the green synthesis of silver nanoparticles and their antibacterial activity. *Appl Surface Sci* 2021;537:147855.
5. Kuppusamy P, Yusoff MM, Maniam GP, Govindan N. Biosynthesis of metallic nanoparticles using plant derivatives and their new avenues in pharmacological applications-An updated report. *Saudi Pharm J* 2016;24(4):473-84.
6. Marslin G, Siram K, Maqbool Q, Selvakesavan RK, Kruszka D, Kachlicki P, *et al.* Secondary metabolites in the green synthesis of metallic nanoparticles. *Materials* 2018;11(6):940.
7. Bhanjadeo MM, Baral B, Subudhi U. Sequence-specific B-to-Z transition in self-assembled DNA: A biophysical and thermodynamic study. *Int J Biol Macromol* 2019;137:337-45.
8. Amatya R, Hwang S, Park T, Chung YJ, Ryu S, Lee J, *et al.* BSA/silver nanoparticle-loaded hydrogel film for local photothermal treatment of skin cancer. *Pharm Res* 2021;38:873-83.
9. Barbir R, Jimenez RR, Martín-Rapún R, Strasser V, Domazet Jurašin D, Dabelić S, *et al.* Interaction of differently sized, shaped, and functionalized silver and gold nanoparticles with glycosylated vs. nonglycosylated transferrin. *ACS Appl Mater Interfaces* 2021;13(23):27533-47.
10. Casals E, Pfaller T, Duschl A, Oostingh GJ, Puentes V. Time evolution of the nanoparticle protein corona. *ACS Nano* 2010;4(7):3623-32.
11. Zhao Z, Li G, Liu QS, Liu W, Qu G, Hu L, *et al.* Identification and interaction mechanism of protein corona on silver nanoparticles with different sizes and the cellular responses. *J Hazardous Mater* 2021;414:125582.
12. Harrman D. Role of free radicals in aging and diseases. *Ann NY Acad Sci* 1992;673(1):126-41.
13. Pradhan B, Patra S, Behera C, Nayak R, Patil S, Bhutia SK, *et al.* *Enteromorpha compressa* extract induces anticancer activity through apoptosis and autophagy in oral cancer. *Mol Biol Rep* 2020;47:9567-78.
14. Young IS, Woodside JV. Antioxidants in health and disease. *J Clin Pathol* 2001;54(3):176-86.
15. Valko M, Leibfritz D, Moncol J, Cronin MT, Mazur M, Telser J. Free radicals and antioxidants in normal physiological functions and human disease. *Int J Biochem Cell Biol* 2007;39(1):44-84.
16. Bastia AK. *In vitro* antioxidant and antibacterial activity of *Scenedesmus obliquus* collected from Similipal biosphere reserve, Odisha, India. *J Indian Bot Soc* 2022;102(3):218-28.
17. Al-Omar MA, Beedham C, Alsarra IA. Pathological roles of reactive oxygen species and their defence mechanisms. *Saudi Pharm J* 2004;12(1):1-8.
18. Shigenaga MK, Hagen TM, Ames BN. Oxidative damage and mitochondrial decay in aging. *Proc Natl Acad Sci* 1994;91(23):10771-8.
19. Liu T, Stern A, Roberts LJ, Morrow JD. The isoprostanes: Novel prostaglandin-like products of the free radical-catalyzed peroxidation of arachidonic acid. *J Biomed Sci* 1999;6(4):226-35.
20. Kumar S, Lemos M, Sharma M, Shriram V. Free radicals and antioxidants. *Adv Appl Sci Res* 2011;2(1):129-35.
21. Harris ED. Copper as a cofactor and regulator of copper, zinc superoxide dismutase. *J Nutr* 1992;122(3):636-40.
22. Harris ED. Regulation of antioxidant enzymes I. *FASEB J* 1992;6(9):2675-83.
23. Trombino S, Serini S, di Nicuolo F, Celleno L, Andò S, Picci N, *et al.* Antioxidant effect of ferulic acid in isolated membranes and intact cells: Synergistic interactions with  $\alpha$ -tocopherol,  $\beta$ -carotene, and ascorbic acid. *J Agric Food Chem* 2004;52(8):2411-20.
24. Hudson BJ, Mahgoub SE. Naturally-occurring antioxidants in leaf lipids. *J Sci Food Agric* 1980;31(7):646-50.
25. Abramovic H, Abram V. Effect of added rosemary extract on oxidative stability of *Camelina sativa* oil. *Acta Agric Slovenica* 2006;87(2):225-61.
26. Kowalski R. GC analysis of changes in the fatty acid

- composition of sunflower and olive oils heated with quercetin, caffeic acid, protocatechuic acid, and butylated hydroxyanisole. *Acta Chromatographica* 2007;18:15-23.
27. Bhuyan PP, Nayak R, Patra S, Abdulabbas HS, Jena M, Pradhan B. Seaweed-derived sulfated polysaccharides; the new age chemopreventives: A comprehensive review. *Cancers* 2023;15(3):715.
  28. Pradhan B, Patra S, Nayak R, Behera C, Dash SR, Nayak S, *et al.* Multifunctional role of fucoidan, sulfated polysaccharides in human health and disease: A journey under the sea in pursuit of potent therapeutic agents. *Int J Biol Macromol* 2020;164:4263-78.
  29. Pradhan B, Patra S, Dash SR, Satapathy Y, Nayak S, Mandal AK, *et al.* *In vitro* antidiabetic, anti-inflammatory and antibacterial activity of marine alga *Enteromorpha compressa* collected from Chilika lagoon, Odisha, India. *Vegetos* 2022;35(3):614-21.
  30. Pradhan B, Nayak R, Patra S, Jit BP, Ragusa A, Jena M. Bioactive metabolites from marine algae as potent pharmacophores against oxidative stress-associated human diseases: A comprehensive review. *Molecules* 2020;26(1):37.
  31. Pradhan B, Nayak R, Patra S, Bhuyan PP, Dash SR, Ki JS, *et al.* Cyanobacteria and algae-derived bioactive metabolites as antiviral agents: Evidence, mode of action, and scope for further expansion: A comprehensive review in light of the SARS-CoV-2 outbreak. *Antioxidants* 2022;11(2):354.
  32. Pradhan B, Nayak R, Patra S, Bhuyan PP, Behera PK, Mandal AK, *et al.* A state-of-the-art review on fucoidan as an antiviral agent to combat viral infections. *Carbohydr Polym* 2022;291:119551.
  33. Pradhan B, Nayak R, Bhuyan PP, Patra S, Behera C, Sahoo S, *et al.* Algal phlorotannins as novel antibacterial agents with reference to the antioxidant modulation: Current advances and future directions. *Marine Drugs* 2022;20(6):403.
  34. Pradhan B, Kim H, Abassi S, Ki JS. Toxic effects and tumor promotion activity of marine phytoplankton toxins: A review. *Toxins* 2022;14(6):397.
  35. Pradhan B, Ki JS. Biological activity of algal derived carrageenan: A comprehensive review in light of human health and disease. *Int J Biol Macromol* 2023;238:124085.
  36. Pradhan B, Bhuyan PP, Patra S, Nayak R, Behera PK, Behera C, *et al.* Beneficial effects of seaweeds and seaweed-derived bioactive compounds: Current evidence and future prospective. *Biocatalysis Agric Biotechnol* 2022;39:102242.
  37. Pradhan B, Ki JS. Antioxidant and chemotherapeutic efficacies of seaweed-derived phlorotannins in cancer treatment: A review regarding novel anticancer drugs. *Phytother Res* 2023;37(5):2067-91.
  38. Zolnik BS, Sadrieh N. Regulatory perspective on the importance of ADME assessment of nanoscale material containing drugs. *Adv Drug Deliv Rev* 2009;61(6):422-7.
  39. Peiris PM, Bauer L, Toy R, Tran E, Pansky J, Doolittle E, *et al.* Enhanced delivery of chemotherapy to tumors using a multicomponent nanochain with radio-frequency-tunable drug release. *ACS Nano* 2012;6(5):4157-68.
  40. Banoee M, Seif S, Nazari ZE, Jafari-Fesharaki P, Shahverdi HR, Moballegh A, *et al.* ZnO nanoparticles enhanced antibacterial activity of ciprofloxacin against *Staphylococcus aureus* and *Escherichia coli*. *J Biomed Mater Res B Appl Biomater* 2010;93(2):557-61.
  41. Radovic-Moreno AF, Lu TK, Puscasu VA, Yoon CJ, Langer R, Farokhzad OC. Surface charge-switching polymeric nanoparticles for bacterial cell wall-targeted delivery of antibiotics. *ACS Nano* 2012;6(5):4279-87.
  42. Wong HL, Wu XY, Bendayan R. Nanotechnological advances for the delivery of CNS therapeutics. *Adv Drug Deliv Rev* 2012;64(7):686-700.
  43. Saad AM, Abdel-Aleem AA, Ghareeb MA, Hamed MM, Abdel-Aziz MS, Hadad AH. *In vitro* antioxidant, antimicrobial and cytotoxic activities and green biosynthesis of silver and gold nanoparticles using *Callistemon citrinus* leaf extract. *J Appl Pharm Sci* 2017;7(6):141-9.
  44. Sood R, Chopra DS. Improved yield of green synthesized crystalline silver nanoparticles with potential antioxidant activity. *Int Res J Pharm* 2017;8(4):100-4.
  45. Bhakya S, Muthukrishnan S, Sukumaran M, Muthukumar M. Biogenic synthesis of silver nanoparticles and their antioxidant and antibacterial activity. *Appl Nanosci* 2016;6:755-66.
  46. Thilagavathi T, Kathiravan G, Srinivasan K. Antioxidant activity and synthesis of silver nanoparticles using the leaf extract of *Limonia acidissima*. *Int J Pharm Bio Sci* 2016;7(4):201-5.
  47. Singhal G, Bhavesh R, Kasariya K, Sharma AR, Singh RP. Biosynthesis of silver nanoparticles using *Ocimum sanctum* (tulsi) leaf extract and screening its antimicrobial activity. *J Nanopart Res* 2011;13:2981-8.
  48. Mohanty AS, Jena BS. Innate catalytic and free radical scavenging activities of silver nanoparticles synthesized using *Dillenia indica* bark extract. *J Colloid Interface Sci* 2017;496:513-21.
  49. Mariam J, Dongre PM, Kothari DC. Study of interaction of silver nanoparticles with bovine serum albumin using fluorescence spectroscopy. *J Fluoresc* 2011;21:2193-9.
  50. Mensor LL, Menezes FS, Leitao GG, Reis AS, Santos TC, Coube CS, *et al.* Screening of Brazilian plant extracts for antioxidant activity by the use of DPPH free radical method. *Phytother Res* 2001;15(2):127-30.
  51. Re R, Pellegrini N, Proteggente A, Pannala A, Yang M, Rice-Evans C. Antioxidant activity applying an improved ABTS radical cation decolorization assay. *Free Radical Biol Med* 1999;26(9-10):1231-7.
  52. Diti PI, Disha PI, Vaishali SN. Preliminary phytochemical screening and evaluation of free radical scavenging activity of *Luffa acutangula* var. amara fruit. *Int J Pharm Erudition* 2012;2(1):34-41.
  53. Ruch RJ, Cheng SJ, Klaunig JE. Prevention of cytotoxicity and inhibition of intercellular communication by antioxidant catechins isolated from Chinese green tea. *Carcinogenesis* 1989;10(6):1003-8.
  54. de Avellar IG, Magalhães MM, Silva AB, Souza LL, Leitão AC, Hermes-Lima M. Reevaluating the role of 1,10-phenanthroline in oxidative reactions involving ferrous ions and DNA damage. *Biochim Biophys Acta* 2004;1675(1-3):46-53.
  55. Priyadarshini S, Sulava S, Bhol R, Jena S. Green synthesis of silver nanoparticles using *Azadirachta indica* and *Ocimum sanctum* leaf extract. *Curr Sci* 2019;117(8):1300-7.
  56. Roche M, Rondeau P, Singh NR, Tarnus E, Bourdon E. The antioxidant properties of serum albumin. *FEBS Lett* 2008;582(13):1783-7.
  57. Bendich A, Machlin LJ, Scandurra O, Burton GW, Wayner DD. The antioxidant role of vitamin C. *Adv Free Radical Biol Med* 1986;2(2):419-44.

58. Preethi K, Vijayalakshmi N, Shamna R, Sasikumar JM. *In vitro* antioxidant activity of extracts from fruits of *Muntingia calabura* Linn. from India. *Pharmacogn J* 2010;2(14):11-8.
  59. Madhumitha B, Abilasha R, Rajeshkumar S. Cytotoxic effect and antioxidant activity of silver nanoparticles synthesised using herbal formulation of *Ocimum sanctum* and *Justicia adhatoda*. *Plant Cell Biotechnol Mol Biol* 2020:1-11.
  60. Pradhan B, Patra S, Behera C, Nayak R, Jit BP, Ragusa A, *et al.* Preliminary investigation of the antioxidant, anti-diabetic, and anti-inflammatory activity of *Enteromorpha intestinalis* extracts. *Molecules* 2021;26(4):1171.
  61. Pradhan B, Patra S, Dash SR, Nayak R, Behera C, Jena M. Evaluation of the anti-bacterial activity of methanolic extract of *Chlorella vulgaris* Beyerinck (Beijerinck) with special reference to antioxidant modulation. *Future J Pharm Sci* 2021;7:1.
  62. Sreelekha E, George B, Shyam A, Sajina N, Mathew B. A comparative study on the synthesis, characterization, and antioxidant activity of green and chemically synthesized SNPs. *Bionano Sci* 2021;11:489-96.
-